Acta Crystallographica Section A
Foundations of Crystallography
ISSN 0108-7673

Received 24 April 2007
Accepted 16 October 2007

A note on Bragg-case *Pendellösung* and dispersion surface

André Authier

Institut de Minéralogie et de Physique des Milieux Condensés, Université P. et M. Curie, 140 rue de Lourmel, F-75015 Paris, France. Correspondence e-mail: aauthier@wanadoo.fr

It is usual to state, since Ewald [*Ann. Phys.* (1917), **54**, 519–597], that Bragg-case *Pendellösung* involves two wavefields belonging to the same branch of the dispersion surface. However, in the Bragg geometry or when crystals are highly absorbing, the dispersion surface can no longer be approximated by the dispersion surface valid for a non-absorbing infinite medium. When considering the real part of the dispersion surface, it is found that the interfering wavefields producing *Pendellösung* in the Bragg geometry belong in fact to different branches. This paradox is explained by noting that the actual dispersion surface in the semi-infinite medium where the wavefields are generated by the incident wave differs from the dispersion surface in an infinite medium.

1. Introduction

In the two-beam approximation, two solutions of the dispersion equation are excited by an incident plane wave. Their interference was called *Pendellösung* by Ewald (1917) in both Laue and Bragg geometry. He noted that in the latter case the two corresponding wavefields are attached to the same branch of the dispersion surface. However, if one plots the real part of the dispersion surface, one finds that these wavefields belong to different branches. The purpose of this note is to discuss this paradox and to provide some reflections on the concept of dispersion surface. This requires revisiting very briefly the bases of dynamical theory.

2. The dispersion equation

The notion of wavefield was introduced by Ewald (1913) in order to describe the optical field in an infinite triply periodic medium 15 years before Bloch (1928). A wavefield is an infinite sum of plane waves of wavevectors $\mathbf{K_o} = \mathbf{OP}$, $\mathbf{K_h} = \mathbf{HP}$, $\mathbf{K_g} = \mathbf{GP}$ *etc*., which are deduced from one another by translations of the reciprocal-lattice vectors

$$\mathbf{K_h} = \mathbf{K_o} - \mathbf{h}, \quad \mathbf{K_g} = \mathbf{K_o} - \mathbf{g} \quad etc.,$$

where $\mathbf{h} = \mathbf{OH}$, $\mathbf{g} = \mathbf{OG}$ *etc*. are reciprocal-lattice vectors. The common extremity of the wavevectors, P, is called the *tiepoint* (Fig. 1). This relation shows that, in an absorbing medium, all the wavevectors of a given wavefield have the same imaginary part and therefore undergo the same absorption. The propagation equation of a wave in an infinite triply periodic medium is equivalent to a infinite set of linear equations (Laue's *Grundgleichungen*), the determinant of which is the *dispersion equation* (*Dispersionsgleichung*, Ewald, 1917). It relates the wavevectors of the wavefield and their frequency. In the two-beam approximation to which we shall limit this note, namely when there is only one couple of wavevectors such that $2\mathbf{K_o}\cdot\mathbf{h} \approx h^2$ (Bragg relation), each wavefield is constituted by two waves only and the dispersion equation is of the form

$$X_o X_h = \frac{k^2}{4} C^2 \chi_h \chi_{\bar{h}}, \tag{1}$$

where $k = 1/\lambda$ is the wavenumber of the radiation propagating in the medium, $C = 1$ or $\cos 2\theta$ is the polarization factor, χ_h and $\chi_{\bar{h}}$ the Fourier coefficients of the dielectric susceptibility (or polarizability) for the h, k, l and $\bar{h}, \bar{k}, \bar{l}$ reflections, respectively, and X_o and X_h are quantities related to $\mathbf{K_o}$ and $\mathbf{K_h}$, respectively. The dispersion equation determines which wavefields may propagate in the infinite medium and the locus of their tiepoints; this is the dispersion surface (*Dispersionsfläche*, Ewald, 1917). The direction of propagation of a wavefield is given by the Poynting vector, $\mathbf{S} = \mathcal{R}e(\mathbf{E} \wedge \mathbf{H}^*)$ (Laue, 1952), where $\mathcal{R}e(\,)$ means real part of $(\,)$. The slope, p, of this propagation direction with respect to the lattice planes is

$$p = \frac{\tan\alpha}{\tan\theta} = \frac{1 - |\xi|^2}{1 + |\xi|^2}, \tag{2}$$

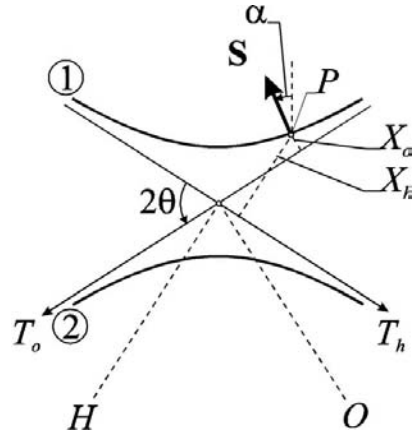

Figure 1
Dispersion surface in an infinite medium (two-beam approximation). T_o, T_h tangents to the spheres of radii nk and centred at O and H, respectively ($k = 1/\lambda$ wavenumber, n index of refraction, O origin of the reciprocal lattice, H node hkl of the reciprocal lattice); **S** Poynting vector of the wavefield of tiepoint P; α angle between **S** and the lattice planes; θ Bragg angle.

where α is the angle between **S** and the lattice planes (Fig. 1), θ the Bragg angle and ξ the ratio between the amplitudes of the two waves constituting the wavefield,

$$\xi = D_h/D_o = 2X_o/kC\chi_{\bar{h}} = kC\chi_h/2X_h.$$

3. The dispersion surface in an infinite medium

In general, if the Bragg angle is neither very small nor close to $\pi/2$, the quantities X_o and X_h can be approximated by the coordinates of the tiepoint with respect to the asymptotes, T_o and T_h, to the spheres of radius nk (n, index of refraction), centred at the reciprocal-lattice points O and H (Fig. 1).

If the medium is non-absorbing, the dispersion surface is real and its intersection with the $\mathbf{K_o}$, $\mathbf{K_h}$ plane is a hyperbola; it has two branches, called 1 and 2 by Ewald (1917). The only wavefields that may propagate in the infinite medium are those whose tiepoints lie on the dispersion surface. Those whose tiepoints lie between the two branches are forbidden; this is the *Bragg* gap, which corresponds to the band gap in the energy diagram. The direction of propagation of the wavefields has been shown by Kato (1958) and by Ewald (1958) using the group velocity to be along the normal to the dispersion surface.

If the medium is absorbing, $\chi_h\chi_{\bar{h}}$ is complex and the dispersion surface is also complex. The dispersion equation (1) can then be split up into two equations, one for the real part and one for the imaginary part. The former is

$$X_{or}X_{hr} = X_{oi}X_{hi} + \frac{k^2}{4}C^2\mathcal{R}e(\chi_h\chi_{\bar{h}}), \tag{3}$$

where X_{or}, X_{oi} and X_{hr}, X_{hi} are the real and imaginary parts of X_o and X_h, respectively. It is the equation of the real part of the dispersion surface.

If the ratio of the imaginary to the real part of χ_h is small enough, equation (3) may be approximated by

$$X_{or}X_{hr} = \frac{k^2}{4}C^2\mathcal{R}e(\chi_h\chi_{\bar{h}}). \tag{4}$$

As noted by Fukamachi *et al.* (2002), this is what is done tacitly in textbooks and reviews (see, for instance, Laue, 1960; Batterman & Cole, 1964), where it is in fact the real part of the dispersion surface that is represented.

The direction of propagation of the wavefields is then approximated by the normal to the real part of the dispersion surface. The plot of the dispersion surface is very useful, for instance in order to follow the path of the wavefields inside the crystal. One can thus find the distribution of wavefields within the Borrmann triangle (Borrmann, 1959) or deduce the curved path of wavefields in a slightly deformed crystal from the displacement of the tiepoint on the dispersion surface [Penning & Polder (1961) and Kato (1963) in the Laue geometry; Bonse (1964) and Gronkowski & Malgrange (1984) in the Bragg geometry]. When approximation (4) does not hold, the path of the wavefields can no longer be approximated by the normal to the real part of the dispersion surface in the infinite medium. Ray tracing is thus not possible in the Bragg geometry if the wavefields have been generated close to the condition of total reflection or if the deformations are large enough for interbranch scattering to occur (Gronkowski & Malgrange, 1984).

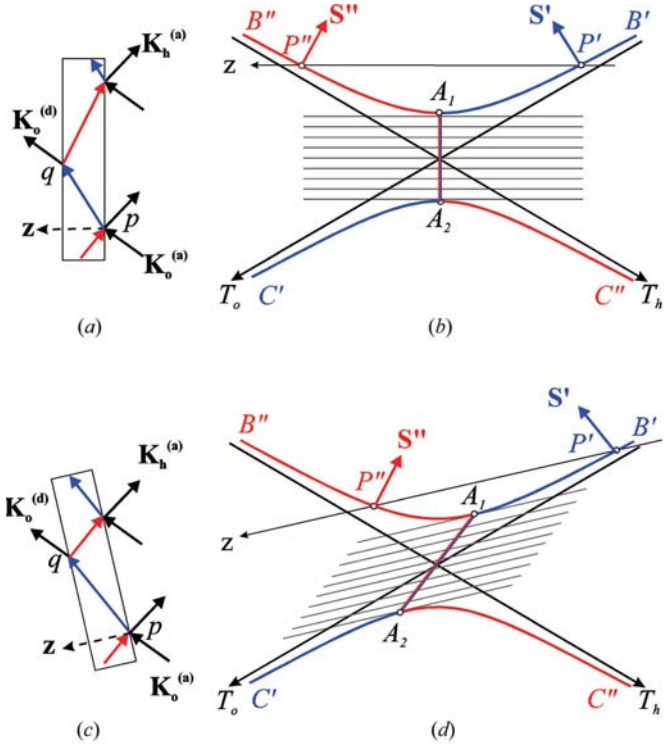

Figure 2
Bragg geometry, non-absorbing crystals. (*a*), (*b*) Symmetric reflection; (*c*), (*d*) asymmetric reflection; (*a*), (*c*) real space, $\mathbf{K_o^{(a)}}$ incident wavevector, $\mathbf{K_h^{(a)}}$ reflected wavevector, $\mathbf{K_o^{(d)}}$ transmitted wavevector; (*b*), (*d*) reciprocal space, real part of the dispersion surface. The two solutions of the dispersion surface and the corresponding paths in direct space are represented in blue and red, respectively. $\mathbf{S}'$, $\mathbf{S}''$ are Poynting vectors at tiepoints P' and P''. Tiepoints A_1 and A_2 correspond to $\eta = -1$ and $+1$, respectively. The hatched regions correspond to the total reflection domain.

4. The dispersion surface in a semi-infinite medium

If the medium is limited by a boundary, the wavefields that actually propagate in the semi-infinite medium are those that are excited by the incident wave. They are determined by applying the condition of the continuity of the tangential component of the wavevectors:

$$\mathbf{K_o} \wedge \mathbf{n} = \mathbf{K_o^{(a)}} \wedge \mathbf{n},$$

where **n** is a unit vector along the normal **pz** to the entrance surface (Figs. 2*a* and 2*c*) and $\mathbf{K_o^{(a)}}$ is the wavevector of the incident plane wave. The coordinates of the tiepoint P are obtained by combining this condition with the dispersion equation (1). In the two-beam approximation, there are two solutions (see, for example, Authier, 2005):

$$X_o = \frac{k|C|\sqrt{\chi_h\chi_{\bar{h}}}}{2\sqrt{|\gamma|}}S(\gamma_h)\left[\eta \pm \sqrt{\eta^2 + S(\gamma_h)}\right] \tag{5}$$

$$X_h = \frac{k|C|\sqrt{|\gamma|}\sqrt{\chi_h\chi_{\bar{h}}}}{2}\left[-\eta \pm \sqrt{\eta^2 + S(\gamma_h)}\right], \tag{6}$$

where γ_o and γ_h are the direction cosines of **pz** with respect to the incident and reflected directions, respectively, $S(\gamma_h)$ is sign of γ_h, $\gamma = \gamma_h/\gamma_o$ is the asymmetry ratio and η is the deviation parameter

$$\eta = \frac{\Delta\theta \sin 2\theta + \chi_o(1-\gamma)/2}{|C|\sqrt{|\gamma|}\sqrt{\chi_h\chi_{\bar{h}}}}$$

($\Delta\theta$ departure from Bragg incidence; χ_o 000 Fourier coefficient of the dielectric susceptibility). When the crystal is absorbing, the deviation

parameter is also complex. The actual dispersion surface in the semi-infinite medium depends on the geometry of the reflection.

4.1. Laue geometry

In the Laue geometry, $S(\gamma_h) = +1$. Unless the imaginary part of the dielectric susceptibility is very large, approximation (4) holds, the real part of the dispersion surface may be approximated by the infinite medium dispersion surface and the tie-points of the two excited wavefields lie on branches (1) and (2), respectively. Their interference, predicted by Ewald in 1917, was first observed for an incident spherical wave by Kato & Lang (1959) and for an incident plane wave by Malgrange & Authier (1965).

4.2. Bragg geometry

In the Bragg geometry, $S(\gamma_h) = -1$, and the two solutions of the dispersion equations, deduced from (5) and (6), are

$$\begin{aligned} X'_o &= -\frac{k|C|\sqrt{\chi_h\chi_{\bar{h}}}}{2\sqrt{|\gamma|}}\left[\eta - S(\eta_r)\sqrt{\eta^2-1}\right] \\ X'_h &= -\frac{k|C|\sqrt{|\gamma|}\sqrt{\chi_h\chi_{\bar{h}}}}{2}\left[\eta + S(\eta_r)\sqrt{\eta^2-1}\right] \end{aligned} \tag{7}$$

$$\begin{aligned} X''_o &= -\frac{k|C|\sqrt{\chi_h\chi_{\bar{h}}}}{2\sqrt{|\gamma|}}\left[\eta + S(\eta_r)\sqrt{\eta^2-1}\right] \\ X''_h &= -\frac{k|C|\sqrt{|\gamma|}\sqrt{\chi_h\chi_{\bar{h}}}}{2}\left[\eta - S(\eta_r)\sqrt{\eta^2-1}\right]. \end{aligned} \tag{8}$$

If the real part, η_r, of the deviation parameter lies within the range $-1 \leq \eta_r \leq +1$, the imaginary part of the coordinates X_o and X_h is large and approximation (4) does not hold; the real part of the dispersion surface may no longer be approximated by the infinite medium dispersion surface.

4.2.1. Non-absorbing crystals. The real part of the dispersion surface is represented in Figs. 2(*b*) and 2(*d*) for a symmetric and an asymmetric reflection, respectively. It consists of two branches, associated with the two solutions of the dispersion equation, (7) and (8), respectively: $B'A_1A_2C'$ for the wavefields propagating towards the bottom of the crystal (blue curve) and $B''A_1A_2C''$ for the wavefields propagating from the bottom of the crystal up towards the entrance surface (red curve). The latter can only be generated by back reflection of the former at the bottom of the crystal (Figs. 2*a* and 2*c*). When the crystal is thick, one wavefield only propagates inside the crystal, the path of which was first observed by Authier (1961).

Parts $B'A_1$ and A_1B'', $C'A_2$ and A_2C'', which do not have corresponding imaginary parts, are exactly superposed on branches 1 and 2 of the infinite medium dispersion surface, respectively. Section A_1A_2, which is common to both branches and corresponds to values of the deviation parameter $-1 \leq \eta \leq +1$, is associated with wavefields that do not exist in the infinite medium but exist in the semi-infinite medium, which is why the dispersion surface is different in the two cases. These wavefields appear within the total reflection domain and are exponentially damped. They do not propagate inside the crystal but along the surface of the crystal, with a zero cross section and are evanescent waves (Cowan, 1985). These evanescent waves have been used by Cowan *et al.* (1986) to produce standing waves for the study of the surface of a germanium crystal. Ewald was well aware of this damped solution when the normal to the crystal surface intercepts the dispersion surface at complex points and spoke in that case of a 'mixed solution' (*eine Lösung vom gemischten Typ*). He did not, however, plot the real part of the dispersion surface, and neither did Laue, but section A_1A_2 was represented sketchily by Fues (1939) and the branch of the real part of the dispersion surface corresponding to wavefields propagating towards the inside of the crystal, $B'A_1A_2C'$ (blue curve), was plotted by Kittel (1971) in the non-absorbing symmetric case.

4.2.2. Absorbing crystals. Real crystals are absorbing and the whole dispersion surface is complex. Its real part is represented in Fig. 3, choosing for better visibility a highly absorbing crystal (symmetric 111 reflection from a GaAs crystal, Mo $K\alpha$ radiation, linear absorption coefficient μ = 319.5 cm^{-1}). There is no longer a total reflection domain and no Bragg gap. Each one of the two branches can be divided up in three sections, the extreme ones, $B'A'_1$, A'_2C', $B''A''_1$ and A''_2C'', lie practically on the infinite medium dispersion surface, and the middle ones, $A'_1A'_2$ and $A''_1A''_2$, replace section A_1A_2 of the no-absorption case. The tiepoints A'_1 and A''_1, A'_2 and A''_2 correspond to values of η_r close to -1 and $+1$, respectively. The real part of the dispersion surface was first calculated by Fukamachi *et al.* (1995, 2002) and Yefanov & Kladko (2006).

There are several interesting points to note.

(*a*) The Bragg-case *Pendellösung* predicted by Ewald is due to the interference between wavefields corresponding to different solutions of the dispersion equation. Their tiepoints P' and P'' lie on the *same* branch of the infinite medium dispersion surface but on *different* branches of the real part of the semi-infinite medium dispersion surface. Bragg-case *Pendellösung* was first observed for an incident

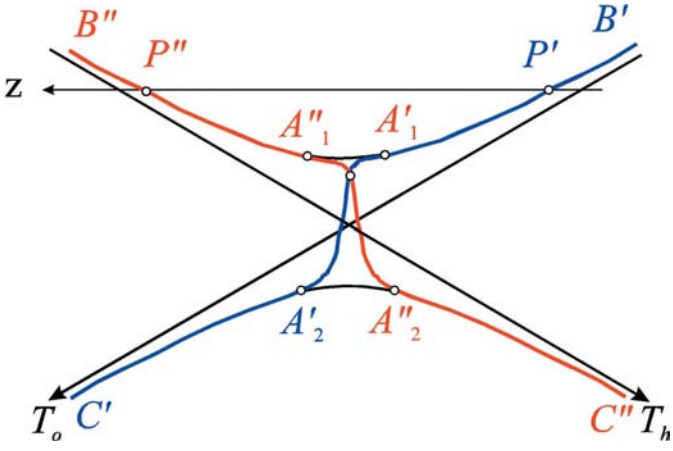

Figure 3
Real part of the dispersion surface – Bragg geometry; GaAs, 111 symmetric reflection, Mo $K\alpha$. The two solutions of the dispersion equation in the bounded crystal are represented in blue and red, respectively. The infinite medium dispersion surface is represented in black. Tiepoints A'_1, A''_1 and A'_2, A''_2 correspond to values of η_r close to -1 and $+1$, respectively.

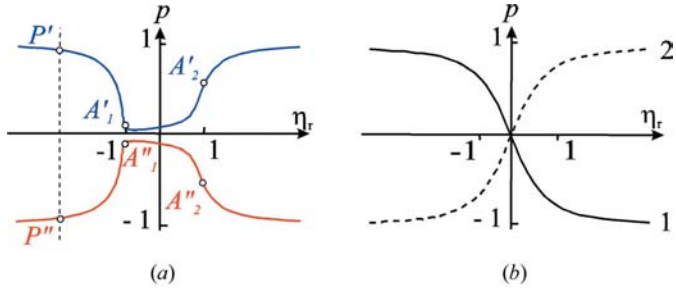

Figure 4
Variations of the slope of the Poynting vectors of the excited wavefields with the deviation parameter; GaAs, symmetric 111 reflection, Mo $K\alpha$; (*a*) Bragg geometry: the blue curve corresponds to wavefields propagating towards the inside of the crystal and the red curve to wavefields propagating from the bottom of the crystal up; P', P'', A'_1, A''_1 are the same tiepoints as in Fig. 3; (*b*) Laue geometry.

plane wave by Batterman & Hildebrandt (1967, 1968) and for an incident spherical wave by Uragami (1969). Lehmann (1974) has shown that it differs from Laue-case *Pendellösung* in that the maxima of the amplitude oscillations depend on the crystal thickness while this is not true in the Laue geometry.

(*b*) Other types of interference such as the Borrmann–Lehmann fringes (Borrmann & Lehmann, 1962, 1963; Lehmann & Borrmann, 1967; Lang *et al.*, 1986, 1990) occur in the Laue–Bragg geometry when the Borrmann triangle is partially intercepted by a lateral face. They are between wavefields having propagated directly and wavefields that have been partially reflected at the lateral surface, namely between wavefields corresponding to the same solution of the dispersion equation. They are not *Pendellösung* fringes.

(*c*) The propagation direction of the wavefields can be approximated by the normal to the real part of the dispersion surface where it does not differ significantly from the infinite medium dispersion surface, but not along the segments $A_1'A_2'$ and $A_1''A_2''$. The variations of the slope of the Poynting vector across the reflection domain, calculated from (2), is represented in Fig. 4(*a*) for the Bragg geometry and absorbing crystals and, for comparison, in Fig. 4(*b*) for the Laue geometry. The slope of the Poynting vector varies continuously from $+1$ ($\tan\alpha = \tan\theta$) to -1 ($\tan\alpha = -\tan\theta$) across the reflection domain in the Laue geometry (spanning the Borrmann fan) while there is a gap of forbidden propagation directions in the Bragg geometry.

5. Concluding remarks

The concept of dispersion surface has been clarified firstly by noting that, in real absorbing crystals, the dispersion surface is complex, in both the transmission and the reflection geometries; it may only be approximated by its real part when its imaginary part is not too large. Secondly, one should distinguish between the case of the infinite medium and that of the semi-infinite medium where boundary conditions have been introduced. For instance, in the Bragg geometry, there are wavefields which exist within the total reflection domain but which are forbidden in the infinite medium; for that reason, the actual dispersion surface in the bounded medium differs from that in the infinite medium.

The tiepoints of the two wavefields which interfere to produce the *Pendellösung* beat effect are associated with different solutions of the dispersion equation. In the Bragg case, they lie on the same branch of the infinite medium dispersion surface but on different branches of the semi-infinite medium dispersion surface.

These considerations are mainly of interest from the viewpoint of the fundamental dynamical theory and have no real bearing on practical issues, although they may be useful when discussing propagation of wavefields in distorted crystals within the total reflection domain, even if this is usually handled using theories which do not involve the dispersion surface.

Stimulating remarks by the referees are gratefully acknowledged.

References

Authier, A. (1961). *C. R. Acad. Sci.* **253**, 1254–1256.
Authier, A. (2005). *Dynamical Theory of X-ray Diffraction.* Oxford University Press.
Batterman, B. W. & Cole, H. (1964). *Rev. Mod. Phys.* **36**, 681–717.
Batterman, B. W. & Hildebrandt, G. (1967). *Phys. Status Solidi*, **23**, K147–K149.
Batterman, B. W. & Hildebrandt, G. (1968). *Acta Cryst.* A**24**, 150–157.
Bloch, F. (1928). *Z. Phys.* **52**, 555–600.
Bonse, U. (1964). *Z. Phys.* **177**, 529–542.
Borrmann, G. (1959). *Beitragen Physikalisch Chemie. 20 Jahrhunderts*, pp. 262–282. Braunschweig: Vieweg and Sohn.
Borrmann, G. & Lehmann, K. (1962). *Direct Observation of Imperfections in Crystals*, pp. 409–414. New York: Interscience Publishers.
Borrmann, G. & Lehmann, K. (1963). *Crystallography and Crystal Perfection*, edited by G. N. Ramachandran, pp. 101–108. London: Academic Press.
Cowan, P. L. (1985). *Phys. Rev. B*, **32**, 5437–5439.
Cowan, P. L., Brennan, S., Jach, T., Bedzyk, M. J. & Materlik, G. (1986). *Phys. Rev. Lett.* **57**, 2399–2402.
Ewald, P. P. (1913). *Phys. Z.* **14**, 465–472.
Ewald, P. P. (1917). *Ann. Phys.* **54**, 519–597.
Ewald, P. P. (1958). *Acta Cryst.* **11**, 888–891.
Fues, E. (1939). *Ann. Phys. (Paris)*, **36**, 209–226.
Fukamachi, T., Negishi, R. & Kawamura, T. (1995). *Acta Cryst.* A**51**, 253–258.
Fukamachi, T., Negishi, R., Zhou, S., Yoshizawa, M. & Kawamura, T. (2002). *Acta Cryst.* A**58**, 552–558.
Gronkowski, J. & Malgrange, C. (1984). *Acta Cryst.* A**40**, 507–514.
Kato, N. (1958). *Acta Cryst.* **11**, 885–887.
Kato, N. (1963). *J. Phys. Soc. Jpn*, **18**, 1785–1791.
Kato, N. & Lang, A. R. (1959). *Acta Cryst.* **12**, 787–794.
Kittel, C. (1971). *Introduction to Solid State Physics.* New York: John Wiley.
Lang, A. R., Kowalski, G., Makepeace, A. P. W. & Moore, M. (1986). *Acta Cryst.* A**42**, 501–510.
Lang, A. R., Kowalski, G. & Makepeace, A. P. W. (1990). *Acta Cryst.* A**46**, 215–227.
Laue, M. von (1952). *Acta Cryst.* **5**, 619–625.
Laue, M. von (1960). *Röntgenstrahl–Interferenzen.* Frankfurt am Main: Akademische Verlagsgesellschaft.
Lehmann, K. (1974). *Phys. Status Solidi A*, **21**, 763–770.
Lehmann, K. & Borrmann, G. (1967). *Z. Kristallogr.* **125**, 234–248.
Malgrange, C. & Authier, A. (1965). *C. R. Acad. Sci.* **261**, 3774–3777.
Penning, P. & Polder, D. (1961). *Philips Res. Rep.* **16**, 419–440.
Uragami, T. (1969). *J. Phys. Soc. Jpn*, **27**, 147–154.
Yefanov, O. M. & Kladko, V. P. (2006). *Met. Phys. New Tech.* **28**, 227–244. (In Russian.)